BL-28A/2021S2-001

μ-ARPES study of charge density wave of Kagome superconductor CsV_3Sb_5

Kosuke NAKAYAMA[1,2,*], Yongkai LI[3,4], Takemi KATO[1], Min LIU[3,4], Zhiwei WANG[3,4], Takashi TAKAHASHI[1,5,6], Yugui YAO[3,4], and Takafumi SATO[1,5,6,7**]

[1]Department of Physics, Graduate School of Science, Tohoku University, Sendai 980-8578, Japan
[2]Precursory Research for Embryonic Science and Technology (PRESTO), Japan Science and Technology Agency (JST), Tokyo 102-0076, Japan
[3]Centre for Quantum Physics, Key Laboratory of Advanced Optoelectronic Quantum Architecture and Measurement (MOE), School of Physics, Beijing Institute of Technology, Beijing 100081, China
[4]Beijing Key Lab of Nanophotonics and Ultrafine Optoelectronic Systems, Beijing Institute of Technology, Beijing 100081, China
[5]Center for Science and Innovation in Spintronics, Tohoku University, Sendai 980-8577, Japan
[6]Advanced Institute for Materials Research (WPI-AIMR), Tohoku University, Sendai 980-8577, Japan
[7]International Center for Synchrotron Radiation Innovation Smart, Tohoku University, Sendai 980-8577, Japan

1 Introduction

Recent discovery of superconductivity with the superconducting transition temperature Tc of 0.93–2.5 K in a family of kagome metals AV_3Sb_5 (AVS) (A = K, Rb, and Cs) [1–3] sparked a great deal of attention, because the realization of superconductivity in kagome metals is very rare and may invoke an unconventional mechanism as inferred from possible symmetry breaking [4–7]. A central issue under intensive debate for the AVS kagome metals is the relationship between the band structure and the mechanism of CDW and superconductivity. Theoretically, the saddle point can promote *f*- or *d*-wave superconducting pairing associated with the scattering with the Q = (π, 0) vector connecting the saddle points, whereas this scattering would also enhance an instability toward CDW (possibly chiral CDW) or unconventional density waves [8–14]. Thus, the interplay between CDW and superconductivity is not straightforward and a fundamental question as to whether the saddle points play a more important role in CDW or superconductivity needs to be answered. Given the multiorbital character of AVS, it is also essential to understand how other bands or orbitals are involved in CDW and superconductivity. In the experimental side, the observation of a CDW gap [4–6,15,16], particularly the large gap on the saddle point of the V $d_{xy/x2-y2}$ band [15,16], supports that the saddle points play a certain role in stabilizing CDW. However, the mechanism of CDW and superconductivity is still far from reaching a consensus. For example, the influence of multiorbital character is yet to be clarified. A promising route to clarify this issue is to control the band energy position relative to E_F through carrier doping because the CDW transition would be sensitive to the saddle point energy and/or the band filling in the simple nesting picture. Carrier doping may also modify a charge balance among multiple orbitals and would be useful to differentiate the contribution of each orbital, as has been utilized to pin down the origin of multiorbital superconductivity and density wave in Fe-based superconductors [17]. However, the carrier-doping effect has been unexplored in AVS due to the lack of an effective means of carrier doping.

Here, we report ARPES study on Cs-dosed CsV_3Sb_5 (CVS) bulk single crystals to experimentally establish the evolution of a Fermi surface (FS) and band structure upon electron doping, and to uncover the orbital-dependent electron-doping effect and suppression of CDW accompanied with the reduction of CDW gaps [18].

2 Experiment

High-quality single crystals of CVS were synthesized with the self-flux method. VUV-ARPES measurements with micro-focused synchrotron light were performed with a DA30 electron analyzer at BL28A [19], as well as SES2002 spectrometers at Tohoku University. The energy resolution was set to be at 35-60 meV at Photon factory and 7 meV at Tohoku University. The angular resolution was set to be 0.2-0.3˚. Crystals were cleaved *in-situ* in an ultrahigh vacuum of ~ 1×10^{-10} Torr.

3 Results and Discussion

Figures 1(a) and 1(b) show the FS mapping for pristine and moderately Cs-dosed (labeled as Cs) samples obtained at T = 120 K above T_{CDW} of pristine CVS (91 K) with 106-eV photons which probe the electronic states at $k_z \sim 0$. In the pristine sample, a circular pocket formed by a parabolic electron band centered at the Γ point [Fig. 1(d)] is recognized. This pocket is attributed to the $5p_z$ band of Sb1 atoms embedded in the kagome-lattice plane [inset of Fig. 1(a)]. At the Brillouin-zone boundary, two features are recognized, one forms a large hexagonal FS centered at the Γ point with mainly V $3d_{xz/yz}$ character of the kagome-lattice band and the other forms a triangular FS centered at the K point with mainly V $3d_{xy/x2-y2}$ character. A side-by-side comparison of Figs. 1(a) and 1(b) reveals that the Γ-centered pocket expands with Cs doping (dashed circles). This is natural because each Cs atom adsorbed on the surface would donate one electron to the CVS bands. The FS expansion is also visualized by a direct comparison of the parabolic band around the Γ point in Figs. 1(c) and 1(d) showing a clear downward shift with Cs dosing. By a quantitative analysis of the experimental band dispersions, the energy shift of the Cs sample with respect to the pristine

one was estimated to be ~0.24 eV, indicating a marked influence of Cs dosing to the surface electronic states of CVS. By determining the location of Fermi wave vector (k_F) points in the 2D k space for the electron pocket [Fig. 1(e)], the FS for the Cs sample was found to be expanded by 65% relative to that of the pristine sample.

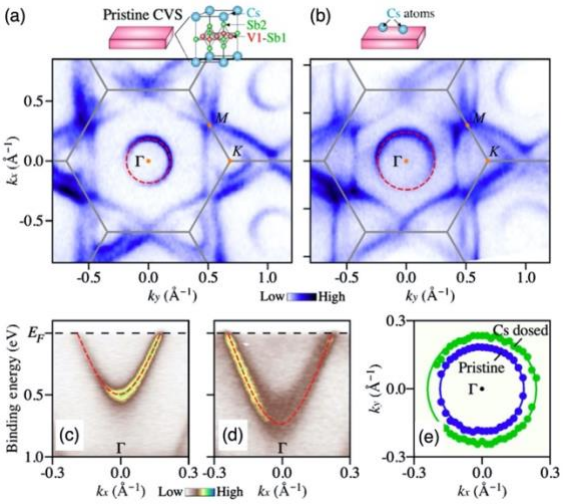

Fig. 1 (a),(b) ARPES-intensity map at E_F plotted as a function of k_x and k_y measured at T = 120 K (above T_{CDW}) with 106-eV photons (corresponding to the k_z ~ 0 plane) for pristine CVS (pristine) and moderately Cs-dosed (Cs) samples, respectively. The inset of (a) shows the crystal structure of CVS. (c),(d) Comparison of the ARPES intensity around the Γ point between pristine and Cs samples. (e) Comparison of the k_F points for the Γ-centered pocket between the two samples.

To examine the energy shift of bands in more detail, we show the APRES intensity along the ΓKM and ΓM cuts in pristine and Cs samples at T = 120 K in Figs. 2(a)–2(d). The ARPES intensity for the pristine sample in Figs. 2(a) and 2(b) signifies the direct correspondence with the calculated bands. For example, besides the Γ-centered electron band with the Sb p_z orbital (labeled as α band) seen in Fig. 1(c), two linearly dispersive bands (β and γ bands) with the V $d_{xz/yz}$ character forming a Dirac-cone-like dispersion between the Γ and K points are identified in the experiment [Fig. 2(a)]. Also, the calculated $d_{xy/x2-y2}$ band (δ band) forming a saddle point pinned almost at E_F, called here the saddle point band, is seen in the experiment as a shallow hole band at the M point. Another calculated $d_{xy/x2-y2}$ band (ε band) that intersects the saddle point band at the K point to form a Dirac point (in the case of negligible SOC) is also seen in the experiment. The ARPES intensity also reproduces the calculated $d_{xz/yz}$ bands topped at ~0.45 eV and near E_F at the M point (ζ and η bands) along the KM cut [Fig. 2(a)], and a shallow electron band (ζ band) and a holelike band with the top of dispersion slightly below EF (ι band) at the M point along the ΓM cut [Fig. 2(b)]. These experimental results show a good agreement with the calculation regarding the number and shape of the band dispersion. All the near-E_F bands predicted in the calculation are also resolved in the Cs sample [Figs. 2(c) and 2(d)] but with a band-dependent energy shift compared with the pristine sample. For instance, the crossing point between the β and γ bands shifts downward by ~0.1 eV after Cs dosing, in disagreement with the downward shift of 0.24 eV for the Γ-centered α band. Furthermore, the crossing point between the δ and ε bands does not show a clear downward shift by Cs dosing [Fig. 2(c)], suggesting the orbital- dependent band shift.

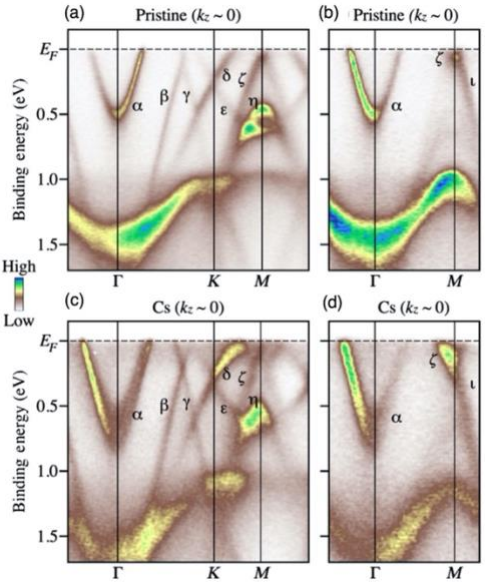

Fig. 2 (a),(b) ARPES intensity as a function of wave vector and binding energy (E_B) in a wide E_B range, measured at T = 120 K along the ΓKM and ΓM lines, respectively, for pristine sample. (c),(d) Same as (a) and (b), respectively, but for Cs sample.

We revealed that Cs dosing leads to an intriguing change in the band structure that is beyond the explanation with the rigid-band model, i.e., the orbital-selective electron doping. We found that the CDW can be completely killed when the $d_{xz/yz}$-derived shallow electron band is pushed away from E_F while keeping the saddle point of the $d_{xy/x2-y2}$ orbital pined almost at E_F, pointing to the importance of the multiorbital effect for understanding the CDW. The present result opens a pathway toward manipulating the CDW and superconducting properties in AV_3Sb_5 through carrier tuning.

Acknowledgements

This work was supported by JST-CREST (No. JPMJCR18T1), JST-PREST (No. JPMJPR18L7), JSPS KAKENHI Grants (No. JP17H01139 and No. JP18H01160). T. K. acknowledges support from GP-Spin at Tohoku University.

References

[1] B. R. Ortiz, L. C. Gomes, J. R. Morey, M. Winiarski, M. Bordelon, J. S. Mangum, I. W. H. Oswald, J. A.

Rodriguez-Rivera, J. R. Neilson, S. D. Wilson, E. Ertekin, T,M. McQueen, and E. S. Toberer, Phys. Rev. Mater. **3**, 3094407 (2019).
[2] B. R. Ortiz, S. M. L. Teicher, Y. Hu, J. L. Zuo, P. M. Sarte, E.C. Schueller, A.M.M. Abeykoon, M.J. Krogstad, S. Rosenkranz, R. Osborn, R. Seshadri, L. Balents, J. He, and S. D. Wilson, Phys. Rev. Lett. **125**, 247002 (2020).
[3] B. R. Ortiz, P. M. Sarte, E. M. Kenney, M. J. Graf, S. M. L. Teicher, R. Seshadri, and S. D. Wilson, Phys. Rev. Mater. **5**, 034801 (2021).
[4] Y.-X. Jiang *et al*., Nat. Mater. **20**, 1353 (2021).
[5] H. Chen, H. Yang, B. Hu, Z. Zhao, J. Yuan, Y. Xing, G. Qian, Z. Huang, G. Li, Y. Ye et al., Nature (London) **599**, 222 (2021).
[6] H. Zhao, H. Li, B. R. Ortiz, S. M. L. Teicher, T. Park, M. Ye, Z. Wang, L. Balents, S. D. Wilson, and I. Zeljkovic, Nature (London) **599**, 216 (2021).
[7] Y. Xiang, Q. Li, Y. Li, W. Xie, H. Yang, Z. Wang, Y. Yao, and H. H. Wen, Nat. Commun. **12**, 6727 (2021).
[8] M. L. Kiesel and R. Thomale, Phys. Rev. B **86**, 121105(R) (2012).
[9] M. L. Kiesel, C. Platt, and R. Thomale, Phys. Rev. Lett. **110**, 126405 (2013).
[10] R. Nandkishore, L. S. Levitov, and A. V. Chubukov, Nat. Phys. **8**, 158 (2012)
[11] H. Tan, Y. Liu, Z. Wang, and B. Yan, Phys. Rev. Lett. **127**, 046401 (2021).
[12] X. Feng, K. Jiang, Z. Wang, and J. Hu, Sci. Bull. **66**, 1384 (2021).
[13] Y.-P. Lin and R. M. Nandkishore, Phys. Rev. B **104**, 045122 (2021).
[14] X. Wu, T. Schwemmer, T. Muller, A. Consiglio, G. Sangiovanni, D. D. Sante, Y. Iqbal, W. Hanke, A. P. Schnyder, M. M. Denner, M. H. Fischer, T. Neupert, and R. Thomale, Phys. Rev. Lett. **127**, 177001 (2021).
[15] X. Zhou, Y. Li, X. Fan, J. Hao, Y. Dai, Z. Wang, Y. Yao, and H.-H. Wen, Phys. Rev. B **104**, L041101 (2021).
[16] K. Nakayama, Y. Li, M. Liu, Z. Wang, T. Takahashi,
Y. Yao, and T. Sato, Phys. Rev. B **104**, L161112 (2021).
[17] P. Richard, T. Sato, K. Nakayama, T. Takahashi, and
H. Ding, Rep. Prog. Phys. **74**, 124512 (2011).
[18] K. Nakayama, Y. Li, T. Kato, M. Liu, Z. Wang, T. Takahashi, Y. Yao, and T. Sato, Phys. Rev. X **12**, 011001 (2022).
[19] M. Kitamura, S. Souma, A. Honma, D. Wakabayashi, H. Tanaka, A.Toyoshima, K. Amemiya, T. Kawakami, K. Sugawara, K. Nakayama, K. Yoshimatsu, H. Kumigashira, T. Sato and K. Horiba, Rev. Sci. Instrum. **93**, 033906 (2022).

* k.nakayama@arpes.phys.tohoku.ac.jp
** t-sato@arpes.phys.tohoku.ac.jp